Mineralogical Magazine (2020), **84**, 691–698
doi:10.1180/mgm.2020.53

CAMBRIDGE UNIVERSITY PRESS

Article

Petrovite, $Na_{10}CaCu_2(SO_4)_8$, a new fumarolic sulfate from the Great Tolbachik fissure eruption, Kamchatka Peninsula, Russia

Stanislav K. Filatov[1]*, Andrey P. Shablinskii[2], Sergey V. Krivovichev[1,2,3], Lidiya P. Vergasova[4] and Svetlana V. Moskaleva[4]

[1]Institute of Earth Sciences, Saint Petersburg State University, University Emb. 7/9., 199034, Saint Petersburg, Russia; [2]Institute of Silicate Chemistry of the Russian Academy of Sciences, Makarova Emb. 2., 199034, Saint Petersburg, Russia; [3]Nanomaterials Research Centre, Kola Science Centre of the Russian Academy of Sciences, Fersmana str. 14., 184209, Apatity, Russia; and [4]Institute of Volcanology and Seismology, Far Eastern Branch of the Russian Academy of Sciences, Piip Boulevard 9, 683006, Petropavlovsk-Kamchatsky, Russia

Abstract

Petrovite, $Na_{10}CaCu_2(SO_4)_8$, is a new sulfate mineral discovered on the Second scoria cone of the Great Tolbachik fissure eruption. The mineral occurs as globular aggregates of tabular crystals up to 0.2 mm in maximal dimension, generally with gaseous inclusions. The empirical formula calculated on the basis of O = 32 is $Na_6(Na_{1.80}K_{0.20})_{\Sigma 2}Na(Ca_{0.82}Na_{0.06}Mg_{0.02})_{\Sigma 0.90}(Cu_{1.84}Mg_{0.16})_{\Sigma 2}(Na_{0.52}\square_{0.48})_{\Sigma 1}S_{8.12}O_{32}$. The crystal-chemical formula is $CuNa_{6-2x}Ca_x(SO_4)_4$, which, for $x \approx 0.5$, results in the idealised formula $Na_{10}CaCu_2(SO_4)_8$. The crystal structure of petrovite was determined using single-crystal X-ray diffraction data; the space group is $P2_1/c$, $a = 12.6346(8)$, $b = 9.0760(6)$, $c = 12.7560(8)$ Å, $\beta = 108.75(9)°$, $V = 1385.1(3)$ Å^3, $Z = 2$ and $R_1 = 0.051$. There are one Cu and six Na sites, one of which is also occupied by the essential amount of Ca. The Cu atom forms five Cu–O bonds in the range 1.980–2.180 Å and two long bonds ≈ 2.9 Å resulting in the formation of the CuO_7 polyhedra, which share corners with SO_4 tetrahedra to form isolated $[Cu_2(SO_4)_8]^{12-}$ clusters. The clusters are surrounded by Na sites, which provide their linkage into a three-dimensional framework. The Mohs' hardness is 4. The mineral is biaxial (+), with $\alpha = 1.498(3)$, $\beta_{calc} = 1.500$, $\gamma = 1.516(3)$ and $2V = 20(10)$ ($\lambda = 589$ nm). The seven strongest lines of the powder X-ray diffraction pattern [*d*, Å (*I*, %) (*hkl*)] are: 7.21(27)(110); 6.25(38)(102); 4.47(31)(212); 3.95(21)(30$\bar{2}$); 3.85(17)(121); 3.70(36)(202); and 3.65(34)(22$\bar{1}$). The mineral is named in honour of Prof Dr Tomas Georgievich Petrov (b. 1931) for his contributions to mineralogy and crystallography and, in particular, for the development of technology for the industrial fabrication of jewellery malachite.

Keywords: petrovite, new mineral, sulfate, crystal structure, fumarolic minerals, Tolbachik, Kamchatka peninsula

(Received 23 April 2020; accepted 22 June 2020; Accepted Manuscript published online: 30 June 2020; Associate Editor: Irina O Galuskina)

Introduction

The fumarole activity of the scoria cones of the Great Tolbachik fissure eruption of 1975–1976 (Fedotov and Markhinin, 1983) and the Tolbachik fissure eruption 2012–2013 (Karpov *et al.*, 2013) is accompanied by intensive exhalation mineralisation, in which sulfate mineralisation plays one of the leading roles. Nowadays, more than 25 new sulfates are described on the Tolbachik volcano, Kamchatka peninsula, Russia, most of which are found on the Second scoria cone of the Great fissure Tolbachik eruption (Pekov *et al.*, 2020). Recently, many new sulfates have been discovered, including Na anhydrous sulfates without additional anions: ivsite, $Na_3H(SO_4)_2$ (Filatov *et al.*, 2013), bubnovaite, $K_2Na_8Ca(SO_4)_6$ (Gorelova *et al.*, 2016), puninite, $Na_2Cu_3O(SO_4)_3$ (Siidra *et al.*, 2017), saranchinaite, $Na_2Cu(SO_4)_2$ (Siidra *et al.*, 2018), itelmenite, $Na_2CuMg_2(SO_4)_4$ (Nazarchuk *et al.*, 2018), belomarinaite, $KNaSO_4$ (Filatov *et al.*, 2019), koryakite, $NaKMg_2Al_2(SO_4)_6$ (Siidra *et al.*, 2020), natroapthitalite, $Na_3K(SO_4)_2$ (Shchipalkina *et al.*, 2020), metathénardite, Na_2SO_4 (Pekov *et al.*, 2019) and dobrovolskiite, $Na_4Ca(SO_4)_3$ (Shablinskii *et al.*, 2020). Reviews on the fumarolic mineralisation of the Tolbachik scoria cones have been provided by Vergasova and Filatov (2012, 2016).

Petrovite has been approved by the Commission on New Minerals, Nomenclature and Classification of the International Mineralogical Association (IMA2018-149b, Filatov *et al.*, 2020). The mineral is named in honour of Prof. Dr. Tomas Georgievich Petrov (b. 1931), a former chairman of the Crystallogenesis Laboratory of the Department of Crystallography, St. Petersburg State University. The scientific activities of Tomas Petrov were devoted to the modelling of crystal growth of minerals (Petrov *et al.*, 1969). He was the first to develop the industrial technology of fabrication of jewellery malachite back in 1977 (Petrov *et al.*, 2013). Tomas Petrov is the author of the two-parameter Alphabet for the Coding of Structural–Chemical Information and RHAT-catalogue of modal mineral compositions of magmatic rocks (Petrov *et al.*, 2012; Petrov, 2014). Type material is stored in the Saint-Petersburg State University Mineralogical Museum, University Emb. 7/9, St. Petersburg 199034, Russia, under catalogue number 1/19696.

*Author for correspondence: Stanislav K. Filatov, Email: filatov.stanislav@gmail.com
Cite this article: Filatov S.K., Shablinskii A.P., Krivovichev S.V., Vergasova L.P. and Moskaleva S.V. (2020) Petrovite, $Na_{10}CaCu_2(SO_4)_8$, a new fumarolic sulfate from the Great Tolbachik fissure eruption, Kamchatka Peninsula, Russia. *Mineralogical Magazine* **84**, 691–698. https://doi.org/10.1180/mgm.2020.53

Fig. 1. A view of the fissure of the micrograben on the west side of the Second Cinder cone of Great Tolbachik fissure eruption (photo taken in 1981).

Occurrence and association

The holotype material was collected in the fumarole located on the west side of the micrograben of the Second scoria cone of the Northern Breakthrough of the Great Tolbachik fissure eruption that occurred in 1975–1976 on the Tolbachik volcano, Kamchatka, Far-Eastern Region, Russia (55°41'N, 160°14'E, 1200 m asl). The specimen was found in 2000. The temperature of the surface of the fumarole was ~200°C. The mineral is a product of exhalative fumarolic activity. The host rock for the mineral is a basalt scoria. The sample was placed into a glass tube, which was closed and waxed and kept under ambient conditions. When the glass tube was opened, no changes of sample were noted.

The graben at the place of the sample collecting was filled with the pyroclastic material (see Fig. 1). The presence of the gas stream was manifested by relatively high temperatures (up to 200°C), newly formed mineral phases and the development of an oxidation process.

The new mineral in the form of blue cryptocrystalline crusts enveloped fine pyroclastic material. Petrovite occurs in association with tiny black scales of tenorite in close intergrowths with transparent green particles of euchlorine, $NaKCu_3O(SO_4)_3$ and white particles of dobrovolskiite, $Na_4Ca(SO_4)_3$. The change of eruptive pyroclastic material was characterised by the wide development of oxidation processes accompanied by the formation of a fine hematite phase. The mineral is relatively stable, which allowed its detailed investigation. The crystallisation of the mineral most likely happened by direct precipitation from volcanic gases.

General appearance and physical properties

The mineral occurs as blue and green globular aggregates of tabular crystals up to 0.2 mm in maximal dimension, generally with gaseous inclusions (Figs 2 and 3). The streak is white and the lustre is vitreous. Fracture is conchoidal. No cleavage or parting was observed. The Mohs' hardness is 4. The calculated density based on the empirical formula and single-crystal unit-cell parameters is 2.80 g/cm^3.

The mineral is optically biaxial (+), with $\alpha = 1.498(3)$, $\beta_{calc} = 1.500$, $\gamma = 1.516(3)$ and $2V = 20(10)$ ($\lambda = 589$ nm). No dispersion or pleochroism was observed. The Gladstone–Dale compatibility index (Mandarino, 1981) based on empirical formula and unit-cell parameters from powder X-ray diffraction data is calculated as $(1 - K_P/K_C) = -0.0007$ (superior).

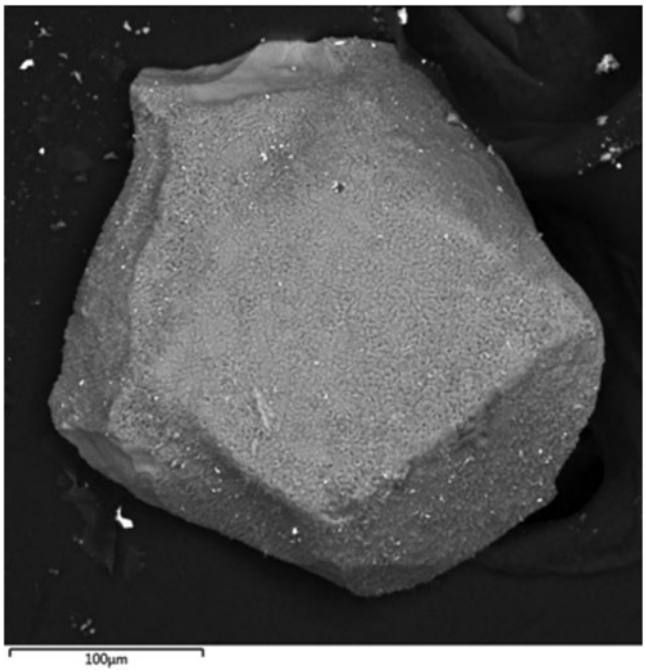

Fig. 2. Scanning electron microscopy image of an individual grain of petrovite. Part of the petrovite sample stored in the Mineralogical Museum of St. Petersburg State University (1/19696).

Chemical composition

The chemical composition of petrovite was studied using a TESCAN "Vega3" electron microprobe equipped with an Oxford Instruments X-max 50 silicon drift energy-dispersive spectroscopy system, operated at 20 kV and 700 pA, with a beam size of 220 nm. Analytical results are given in Table 1. The data processing was done using Aztec software and an X-MAX-80 mm^2 detector (Institute of Volcanology and Seismology, Petropavlovsk-Kamchatsky, Russia). The empirical formula calculated on the basis of 32 O atoms per formula unit is $Na_{9.38}Ca_{0.82}K_{0.20}Cu_{1.84}Mg_{0.18}S_{8.12}O_{32}$. The formula that takes into account the site assignment is $Na_3(Na,K)(Cu,Mg)(Na,Ca,Mg)(Na,\square)(SO_4)_4$. The idealised formula derived from the combination of chemical and structural studies (see below) is $Na_{10}Cu_2Ca(SO_4)_8$.

Powder X-ray diffraction

The powder X-ray diffraction data were collected using a Rigaku R-AXIS RAPID II (Gandolfi mode with Co$K\alpha$) and handled using the domestic software (Britvin *et al.*, 2017). Petrovite is monoclinic, $P2_1/c$, $a = 12.6346(8)$, $b = 9.0760(6)$, $c = 12.7560(8)$ Å, $\beta = 110.75(9)°$, $V = 1385.1(3)$ Å^3 and $Z = 2$.

The measured and calculated powder-diffraction data are given in Table 2. The seven strongest lines are [d, Å (I, %) (hkl)]: 7.21 (27)(110); 6.25(38)(102); 4.47(31)(212); 3.95(21)(30$\bar{2}$); 3.85(17)(121); 3.70(36)(202); and 3.65(34)(22$\bar{1}$).

Single-crystal X-ray diffraction

The single-crystal X-ray diffraction data were collected using a Bruker Smart APEX II diffractometer equipped with a CCD detector using Mo$K\alpha$ radiation. A hemisphere of three-dimensional data was collected using a frame width of 0.5° in

https://doi.org/10.1180/mgm.2020.53 Published online by Cambridge University Press

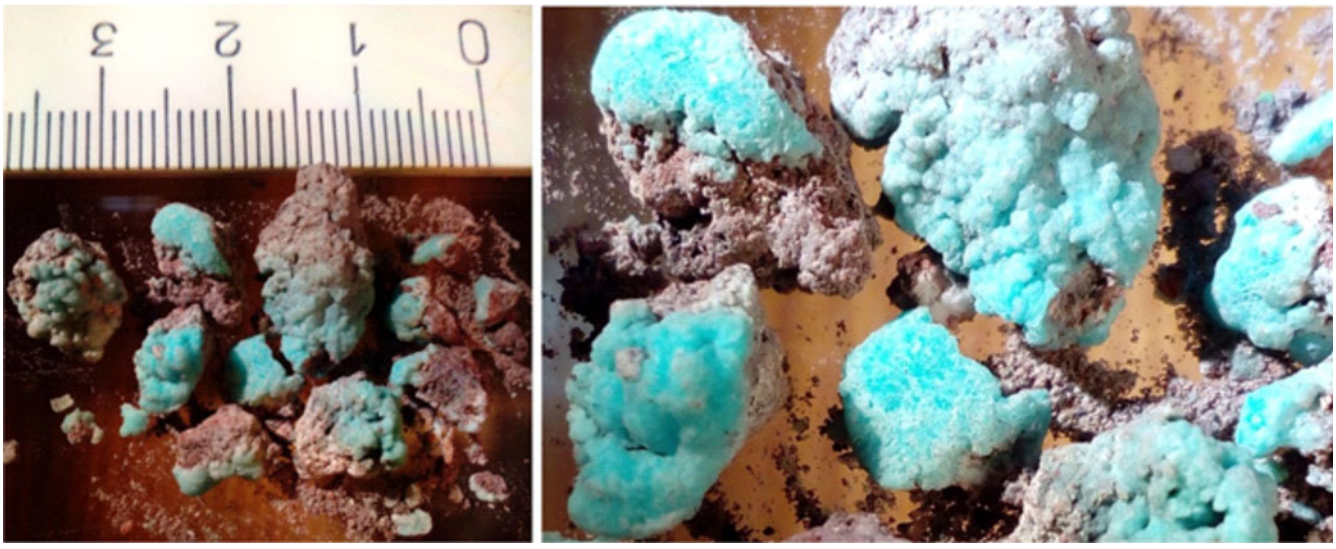

Fig. 3. Blue cryptocrystalline crusts of petrovite enveloped by fine pyroclastic material. Parts of the petrovite sample stored in the Mineralogical Museum of St. Petersburg State University (1/19696).

Table 1. Chemical composition of petrovite (wt.%).

Constituent	Mean	Range	S.D.	Probe standard
Na_2O	25.03	24.47–25.97	0.45	NaCl
K_2O	0.80	0.69–1.10	0.12	sanidine
CaO	3.91	3.44–4.98	0.48	diopside
CuO	12.64	11.86–13.33	0.44	Cu
MgO	0.59	0.00–0.97	0.28	MgO
SO_3	55.98	55.31–56.85	0.50	ZnS
Total	98.97			

S.D. – standard deviation

ω, with 60 s used to acquire each frame. The data were corrected for Lorentz, polarisation and background effects using the Bruker program *APEX*. A semi-empirical absorption-correction based on the intensities of equivalent reflections was applied in the *SADABS* program.

The crystal structure of petrovite was solved by charge flipping and refined on the basis of 2470 unique observed reflections using the *JANA2006* program suite (Petříček *et al.*, 2006). The observed isotropic displacement parameter of the Na6 site was too high (0.327 $Å^2$), so the site was split into two mutually exclusive sites

Table 2. Powder X-ray diffraction data (*d* in Å) for petrovite.

I_{obs}	I_{calc}	d_{obs}	d_{calc}	*h k l*	I_{obs}	I_{calc}	d_{obs}	d_{calc}	*h k l*	I_{obs}	I_{calc}	d_{obs}	d_{calc}	*h k l*
1	2	11.95	11.96	1 0 0	20	22	2.791	2.790	2 1 3	2	1	1.767	1.766	7 1 $\bar{2}$
100	100	7.24	7.26	0 1 1	12	6	2.785	2.783	3 1 2	4	3	1.745	1.739	1 4 4
27	**26**	**7.21**	**7.23**	**1 1 0**	2	2	2.753	2.760	3 1 $\bar{4}$	4	3	1.738	1.735	4 4 1
38	**38**	**6.25**	**6.26**	**1 0 $\bar{2}$**	7	8	2.741	2.750	4 1 $\bar{3}$	5	4	1.726	1.719	1 3 $\bar{6}$
1	1	5.98	5.98	2 0 0	10	11	2.731	2.727	1 0 4	2	1	1.724	1.715	5 2 $\bar{6}$
1	2	5.11	5.13	2 1 $\bar{1}$	48	52	2.600	2.610	2 3 $\bar{2}$	3	2	1.720	1.712	6 2 $\bar{5}$
2	2	5.02	5.03	0 1 2	37	40	2.571	2.580	4 0 $\bar{4}$	2	1	1.690	1.681	6 1 $\bar{6}$
8	4	4.52	4.54	0 2 0	2	2	2.394	2.393	5 0 0	2	1	1.669	1.667	3 4 3
31	**32**	**4.47**	**4.49**	**2 1 $\bar{2}$**	2	2	2.326	2.325	4 2 1	4	2	1.668	1.662	1 2 $\bar{7}$
1	1	3.98	3.99	3 0 0	3	2	2.323	2.323	2 1 4	6	4	1.655	1.649	0 4 5
21	**24**	**3.95**	**3.97**	**3 0 $\bar{2}$**	4	4	2.235	2.243	4 2 $\bar{4}$	4	3	1.646	1.643	5 4 0
17	**22**	**3.85**	**3.87**	**1 2 1**	4	3	2.169	2.169	1 4 1	3	3	1.614	1.617	4 1 5
9	6	3.84	3.85	1 1 $\bar{3}$	4	2	2.134	2.141	5 2 $\bar{3}$	3	3	1.611	1.615	5 1 4
14	18	3.81	3.82	3 1 $\bar{1}$	2	2	2.126	2.132	0 2 5	3	2	1.603	1.606	3 0 6
36	**38**	**3.70**	**3.70**	**2 0 2**	2	2	2.124	2.127	4 3 0	3	3	1.593	1.586	3 0 $\bar{8}$
3	3	3.68	3.68	0 1 3	2	3	2.113	2.116	4 2 2	3	2	1.552	1.545	2 4 $\bar{6}$
15	15	3.66	3.67	1 2 $\bar{2}$	6	3	2.100	2.102	3 3 2	3	2	1.548	1.545	7 3 $\bar{2}$
34	**35**	**3.65**	**3.66**	**2 2 $\bar{1}$**	2	3	2.022	2.025	6 1 $\bar{1}$	2	1	1.544	1.536	4 1 $\bar{8}$
4	5	3.64	3.65	2 1 $\bar{3}$	10	11	1.929	1.934	2 4 2	2	2	1.542	1.538	6 4 $\bar{2}$
2	3	3.40	3.41	2 2 $\bar{2}$	5	7	1.922	1.925	2 2 $\bar{6}$	2	1	1.534	1.538	2 5 3
5	6	3.10	3.10	1 2 $\bar{3}$	6	4	1.910	1.910	6 2 $\bar{2}$	2	2	1.536	1.529	4 5 $\bar{3}$
21	22	2.99	2.99	2 2 $\bar{3}$	2	2	1.887	1.889	6 2 $\bar{1}$	3	2	1.530	1.527	8 1 $\bar{4}$
2	3	2.99	2.99	4 0 0	8	4	1.850	1.849	4 0 4	4	2	1.520	1.525	7 0 2
4	4	2.98	2.99	3 2 $\bar{2}$	2	2	1.842	1.838	0 2 6	4	2	1.513	1.512	2 3 6
17	18	2.924	2.933	1 3 0	2	2	1.824	1.826	6 2 0	2	1	1.512	1.513	3 2 6
3	2	2.889	2.897	3 0 $\bar{4}$	5	4	1.811	1.803	5 3 $\bar{4}$	2	2	1.512	1.509	0 0 8
26	29	2.866	2.866	2 2 2	2	2	1.807	1.802	4 4 0	4	2	1.512	1.504	0 6 0
26	14	2.864	2.865	0 1 4	7	5	1.795	1.785	0 5 1	3	2	1.504	1.508	6 2 3
28	30	2.837	2.840	4 1 0	6	6	1.788	1.780	2 1 $\bar{7}$	5	3	1.504	1.506	6 3 2

The seven strongest lines are given in bold

https://doi.org/10.1180/mgm.2020.53 Published online by Cambridge University Press

Table 3. Crystal data, data collection information and structure refinement details for petrovite.

Crystal data	
Chemical formula	$Na_{9.92}Cu_{1.77}Ca_{0.94}Mg_{0.23}K_{0.20}(SO_4)_8$
Crystal size (mm)	0.075 × 0.06 × 0.05
Crystal system, space group	Monoclinic, $P2_1/c$
Temperature (K)	293
a, *b*, *c* (Å)	12.6153(16), 9.0264(12), 12.7166(16)
α, β, γ (°)	90, 108.311(3), 90
V (Å^3)	1374.7(3)
Z	2
M_r	1160.0
Calculated density (g/cm^3)	2.802
μ (mm^{-1})	2.482
Data collection	
Diffractometer	Bruker Kappa APEX DUO
Radiation type, wavelength (Å)	Mo*K*α, λ = 0.71069
Absorption correction	Empirical (using intensity measurements)
T_{min}, T_{max}	0.820, 0.870
No. of measured, independent and observed [$I > 3\sigma(I)$] reflections	26637, 3114, 2470
R_{int}	0.026
$(\sin\theta/\lambda)_{max}$ (Å^{-1})	0.7
Indices range of *h*, *k*, *l*	$-22 \le h \le 23, -13 \le k \le 15, -21 \le l \le 23$
Refinement	
Number of reflections, parameters, restraints.	3114, 255, 0
R (obs), *wR* (obs)	0.051, 0.061
GoF (obs)	3.03
$\Delta\rho_{max}$, $\Delta\rho_{min}$ (e^- Å^{-3})	0.85, −0.61

with reasonable displacement parameters. Crystallographic data and refinement parameters, atomic coordinates and isotropic displacement parameters, atomic anisotropic displacement parameters and selected interatomic distances are summarised in Tables 3–5. The crystallographic information files have been deposited with the Principal Editor of *Mineralogical Magazine* and are available as Supplementary material (see below).

Crystal structure

The crystal structure of petrovite belongs to a new structure type. It contains four symmetrically independent SO_4 tetrahedra with the average <S–O> bond lengths in the range 1.45–1.47 Å, in general agreement with the average value of 1.475 Å given for sulfate minerals (Hawthorne *et al.*, 2000). The short S–O bonds in several tetrahedra can be explained by libration effects, typical for the crystal structures with statistical or dynamical disorder.

There are six Na and one Cu sites with different occupancies. The Cu atom forms five Cu–O bonds in the range 1.980–2.180 Å and two long bonds ≈ 2.9 Å resulting in the formation of the CuO_7 polyhedra with [5+2] coordination of Cu (Fig. 4a). The Cu site is predominantly occupied by Cu (89%) with the admixture of Mg (11%). This type of coordination geometry of Cu^{2+} cations is rather unusual, but was described previously in the crystal structures of saranchinaite, $Na_2Cu(SO_4)_2$ (Siidra *et al.*, 2018; Kovrugin *et al.*, 2019), the high pressure phase (II) $CuGeO_3$ (Yoshiasa *et al.*, 2000) and $Cu_3(Hbtc)(btc)(bpy)_2$ (Nadeem *et al.*, 2010). After saranchinaite, petrovite is the second mineral with heptacoordinated Cu^{2+}.

The CuO_7 polyhedra share corners with SO_4 tetrahedra to form isolated $[Cu_2(SO_4)_8]^{12-}$ anionic clusters shown in Fig. 4b, which are the fundamental building blocks for the structure of petrovite. The arrangement of the clusters in shown in Fig. 4c. The four Na sites, Na2, Na3, Na4 and Na5, are fully occupied by Na. In the Na1 site, the essential amount of Ca is present (*ca.* 47%), which explains its high bond-valence sum (see below).

Table 4. Atomic coordinates and displacement parameters (Å^2) for petrovite.

Atom	Occupancy	*x/a*	*y/b*	*z/c*	U_{eq}	U^{11}	U^{22}	U^{33}	U^{12}	U^{13}	U^{23}
Cu	$Cu_{0.89}Mg_{0.11}$	0.18775(4)	0.09010(5)	0.05695(4)	0.03063(17)	0.0249(3)	0.0352(3)	0.0285(3)	−0.00237(15)	0.00366(17)	0.00250(14)
Na1	$Na_{0.53}Ca_{0.47}$	0.43241(6)	−0.58365(7)	0.30936(6)	0.0178(2)	0.0188(3)	0.0171(3)	0.0155(3)	−0.0040(2)	0.0027(3)	−0.0026(2)
S1	S	0.34743(8)	−0.10480(10)	−0.02775(8)	0.0369(3)	0.0348(4)	0.0432(5)	0.0310(4)	0.0010(3)	0.0078(3)	−0.0054(3)
S2	S	−0.03339(8)	0.09005(10)	−0.14717(7)	0.0348(3)	0.0306(4)	0.0461(5)	0.0242(4)	−0.0013(3)	0.0034(3)	0.0008(3)
S3	S	0.19689(9)	0.42089(10)	0.09920(11)	0.0463(4)	0.0367(5)	0.0329(5)	0.0673(7)	0.0013(3)	0.0134(5)	0.0024(4)
S4	S	0.39105(7)	0.08439(8)	0.28612(6)	0.0286(2)	0.0277(4)	0.0301(4)	0.0260(3)	0.0000(3)	0.0055(3)	−0.0022(2)
Na2	Na	0.43690(12)	0.27898(18)	0.05467(12)	0.0408(4)	0.0297(6)	0.0496(8)	0.0366(6)	0.0001(6)	0.0011(5)	−0.0009(6)
Na3	Na	0.16368(17)	0.3287(3)	−0.16980(16)	0.0754(9)	0.0424(10)	0.126(2)	0.0507(9)	−0.0159(11)	0.0053(8)	0.0363(11)
Na4	$Na_{0.90}K_{0.10}$	0.28512(18)	−0.24860(15)	0.21027(14)	0.0600(6)	0.0765(12)	0.0277(7)	0.0569(9)	0.0050(6)	−0.0061(8)	0.0029(6)
Na5	Na	0.92753(11)	0.27643(14)	0.08026(10)	0.0313(4)	0.0300(6)	0.0293(6)	0.0269(5)	0.0077(5)	−0.0020(4)	−0.0056(4)
Na6	$Na_{0.30}$	−0.107(6)	0.415(3)	−0.2629(18)	0.120(11)	0.13(2)	0.125(14)	0.095(10)	0.000(12)	0.018(12)	−0.040(10)
Na6'	$Na_{0.23}$	−0.137(2)	0.424(3)	−0.268(2)	0.092(10)	0.051(11)	0.091(11)	0.14(2)	−0.002(6)	0.040(9)	0.034(17)
O1	O	0.2836(3)	0.0292(4)	0.2063(2)	0.0488(10)	0.0347(14)	0.0647(19)	0.0404(13)	−0.0160(13)	0.0022(11)	−0.0017(13
O2	O	0.3640(4)	0.3514(5)	−0.1212(3)	0.0718(16)	0.059(2)	0.084(3)	0.072(2)	0.003(2)	0.0200(19)	0.037(2)
O3	O	0.0820(3)	0.1465(4)	−0.0891(3)	0.0562(12)	0.0449(17)	0.0596(19)	0.0565(18)	−0.0136(15)	0.0051(14)	0.0164(15)
O4	O	0.3196(3)	0.0503(3)	−0.0164(3)	0.0531(12)	0.059(2)	0.0411(15)	0.0569(17)	−0.0001(13)	0.0147(15)	0.0074(13)
O5	O	0.1173(5)	0.3551(5)	0.1477(4)	0.085(2)	0.101(4)	0.075(3)	0.089(3)	−0.022(3)	0.045(3)	−0.006(2)
O6	O	−0.0251(4)	−0.0635(4)	−0.1770(4)	0.0636(14)	0.055(2)	0.063(2)	0.071(2)	−0.0048(16)	0.0173(18)	−0.0036(17)
O7	O	0.4685(5)	−0.0335(5)	0.3147(4)	0.0891(19)	0.096(4)	0.072(2)	0.076(3)	0.039(3)	−0.005(2)	−0.010(2)
O8	O	0.2862(4)	−0.5068(5)	0.1891(4)	0.0846(19)	0.087(3)	0.055(2)	0.106(3)	−0.015(2)	0.023(2)	−0.039(2)
O9	O	−0.0875(4)	0.1796(6)	−0.2443(3)	0.0742(16)	0.075(3)	0.098(3)	0.0495(18)	0.020(2)	0.0194(18)	0.0379(19)
O10	O	0.4196(4)	−0.1614(4)	0.0780(3)	0.0691(15)	0.100(3)	0.0475(18)	0.0484(17)	0.0204(19)	0.0065(18)	0.0103(14)
O11	O	0.0984(3)	−0.0964(4)	0.0686(3)	0.0540(12)	0.100(3)	0.0475(18)	0.0484(17)	0.0204(19)	0.0065(18)	0.0103(14)
O12	O	0.2482(4)	0.2994(5)	0.0543(4)	0.0735(16)	0.058(2)	0.064(2)	0.101(3)	−0.0113(18)	0.029(2)	−0.019(2)
O13	O	0.4334(5)	0.2068(6)	0.2306(3)	0.0883(19)	0.105(4)	0.110(3)	0.0427(16)	−0.061(3)	0.012(2)	0.0058(19)
O14	O	0.1475(5)	0.5249(7)	0.0189(8)	0.141(4)	0.085(4)	0.110(4)	0.226(8)	0.029(3)	0.046(5)	0.120(5)
O15	O	0.2486(4)	−0.1934(6)	−0.0734(5)	0.096(2)	0.065(3)	0.081(3)	0.139(5)	−0.019(2)	0.030(3)	−0.027(3)
O16	O	0.4041(6)	−0.1299(9)	−0.1068(4)	0.131(3)	0.144(5)	0.206(6)	0.052(2)	0.128(5)	0.042(3)	0.036(3)

https://doi.org/10.1180/mgm.2020.53 Published online by Cambridge University Press

Table 5. Selected interatomic distances (Å) for petrovite.

Cu1–O1	1.982(3)	Na1–O10	2.086(4)	Na2–O2	2.232(4)	Na3–O3	2.342(5)
Cu1–O3	1.983(3)	Na1–O8	2.109(5)	Na2–O16	2.332(7)	Na3–O6	2.379(4)
Cu1–O12	2.042(5)	Na1–O13	2.142(7)	Na2–O13	2.344(5)	Na3–O2	2.414(6)
Cu1–O11	2.057(4)	Na1–O16	2.285(9)	Na2–O12	2.386(4)	Na3–O12	2.724(5)
Cu1–O4	2.181(5)	Na1–O7	2.344(7)	Na2–O7	2.409(5)	Na3–O5	2.762(5)
<Cu1–O>$_5$	2.05	Na1–O2	2.801(6)	Na2–O4	2.535(3)	Na3–O1	2.813(5)
Cu1–O5	2.913(5)	<Na1–O>$_6$	2.29	<Na2–O>$_6$	2.37	<Na3–O>$_6$	2.57
Cu1–O6	2.927(5)						
<Cu1–O>$_7$	2.30						
Na4–O8	2.347(5)	Na5–O14	2.226(7)	Na6–O6	2.05(4)	Na6'–O9	2.29(2)
Na4–O1	2.508(4)	Na5–O15	2.320(6)	Na6–O9	2.14(2)	Na6'–O15	2.32(2)
Na4–O16	2.583(6)	Na5–O9	2.331(5)	Na6–O15	2.48(2)	Na6'–O6	2.36(3)
Na4–O9	2.732(6)	Na5–O5	2.384(6)	Na6–O5	2.57(3)	Na6'–O5	2.48(3)
Na4–O11	2.831(4)	Na5–O6	2.402(4)	Na6–O8	2.83(4)	Na6'–O8	2.51(3)
Na4–O10	2.850(6)	Na5–O11	2.438(4)	Na6–O3	2.89(3)	Na6'–O3	2.93(3)
Na4–O7	2.993(5)	<Na5–O>$_6$	2.35	<Na6–O>$_6$	2.49	<Na6'–O>$_6$	2.48
<Na4–O>$_7$	2.69						
S1–O16	1.423(7)	S2–O6	1.449(4)	S3–O14	1.383(7)	S4–O7	1.413(5)
S1–O15	1.441(5)	S2–O9	1.455(4)	S3–O5	1.460(8)	S4–O2	1.447(5)
S1–O10	1.459(4)	S2–O11	1.480(4)	S3–O12	1.476(5)	S4–O13	1.497(6)
S1–O4	1.461(4)	S2–O3	1.500(4)	S3–O8	1.481(4)	S4–O1	1.500(3)
<S1–O>$_4$	1.45	<S2–O>$_4$	1.47	<S3–O>$_4$	1.45	<S4–O1>$_4$	1.46

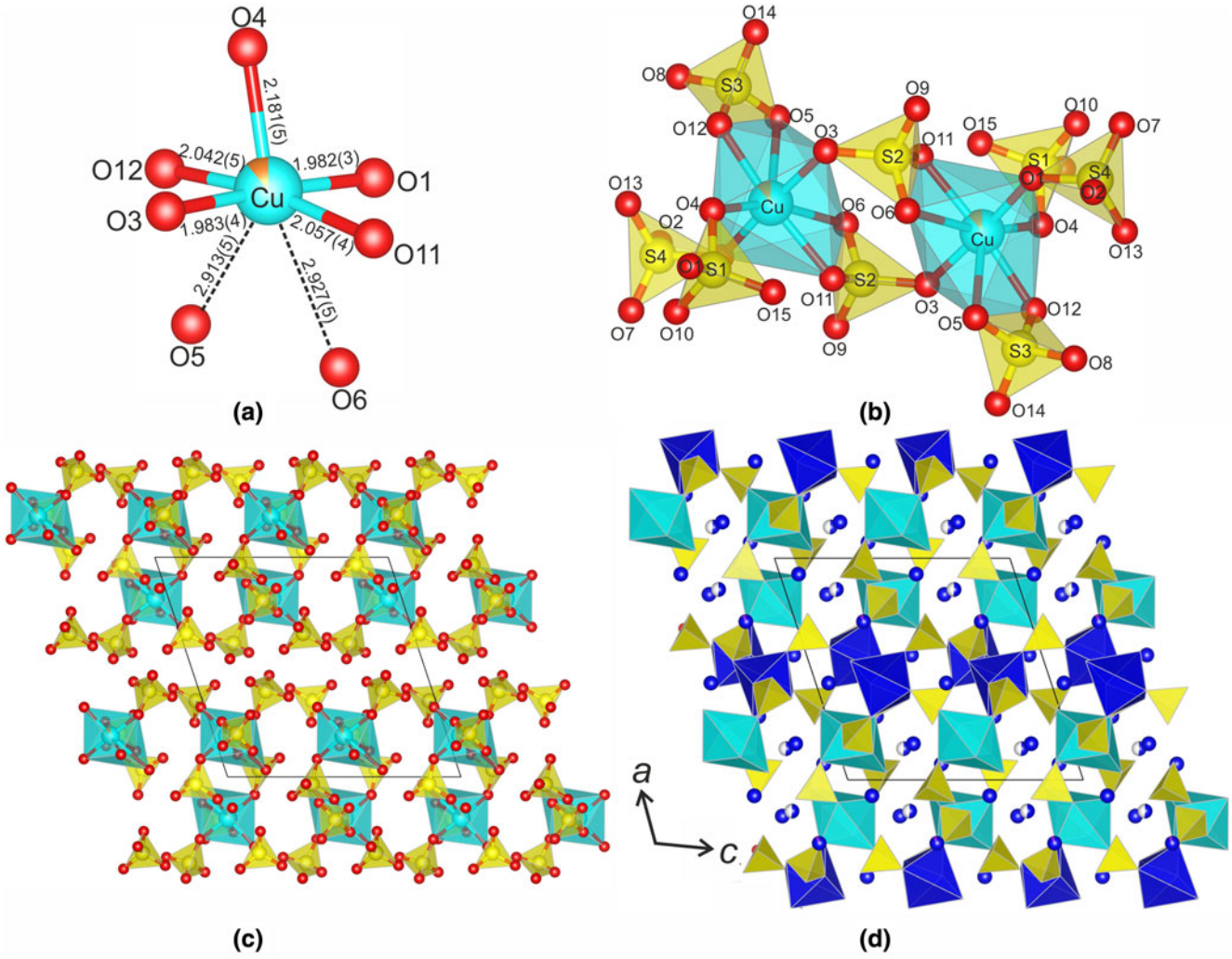

Fig. 4. The crystal structure of petrovite: (*a*) CuO_7 polyhedron; (*b*) the $[Cu_2(SO_4)_8]^{12-}$ cluster; (*c*) arrangement of the $Cu_2(SO_4)_8$ clusters in the structure; and (*d*) three-dimensional framework of the crystal structure.

https://doi.org/10.1180/mgm.2020.53 Published online by Cambridge University Press

Table 6. Bond-valence analysis (vu = valence units) for petrovite.

	S1	S2	S3	S4	Cu1	Na1	Na2	Na3	Na4	Na5	Na6	Na6'	Σ
O1				1.40	0.44			0.05	0.20				2.09
O2				1.61		0.06	0.22	0.14					2.03
O3		1.40			0.44			0.17			0.01	0.01	2.03
O4	1.55				0.26		0.10						1.91
O5			1.56		0.04			0.06		0.15	0.02	0.03	1.86
O6		1.60			0.03			0.15		0.14	0.11	0.04	2.07
O7				1.77		0.22	0.14		0.01				2.14
O8			1.47			0.41			0.26		0.01	0.02	2.17
O9		1.58							0.15	0.17	0.09	0.04	2.03
O10	1.56					0.44			0.13				2.13
O11		1.48			0.36				0.14	0.13			2.11
O12			1.49		0.38		0.15	0.06					2.08
O13				1.41		0.38	0.17						1.96
O14			1.92							0.23			2.15
O15	1.64									0.18	0.03	0.04	1.89
O16	1.72					0.26	0.17		0.18				2.33
Σ	6.48	6.06	6.44	6.19	1.95*	1.77*	0.95	0.61	1.08	1.00	0.28**	0.18**	

* The site is occupied by two cations
** The site is partially occupied

The Na6 site is only partially occupied (53%). The Na1, Na2, Na3, Na5, Na6 and Na6' atoms are surrounded by six O atoms each, forming distorted octahedra with the average bond lengths equal to 2.29, 2.37, 2.57, 2.35, 2.49 and 2.48 Å, respectively. The Na4 site is coordinated by seven O atoms with the Na4–O bond lengths in the range 2.347–2.993 Å.

The petrovite structure can also be described as a three-dimensional framework, taking into account the essential occupancy of the Na1 site by Ca^{2+} cations. In this description, the $[Cu_2(SO_4)_8]^{12-}$ clusters are linked by $Na1O_6$ octahedra, forming a porous three-dimensional framework (Fig. 4*d*) with cavities occupied by Na^+ cations.

The bond-valence calculations were performed using empirical parameters taken from Brown and Altermatt (1985). The results are presented in Table 6. The high bond-valence sums of the S sites and the Na1 site are significantly overbonded, whereas the bond valence sum for Na3 is 0.61 valence units (vu). The deviation of the bond-valence sums from the expected values may be explained by the structural and positional disorder as well as the high ionic mobility of the Na atoms (see below).

Discussion

Taking into account the essential admixture of Ca in the Na1 site, and the low occupancy of the Na6 site, the crystal chemical formula of petrovite can be written as $Na_{6-2x}Ca_xCu(SO_4)_4$. For petrovite, $x \approx 0.5$, which results in the idealised formula $Na_{10}CaCu_2(SO_4)_8$. However, at least theoretically, the x parameter may vary, resulting in different mineral species. For instance, for $x = 0$, 1, 1.5 and 2, the idealised formulae are $Na_6Cu(SO_4)_4$, $Na_4CaCu(SO_4)_4$, $Na_6Ca_3Cu_2(SO_4)_8$ and $Na_2Ca_2Cu(SO_4)_4$, respectively. The $x = 2$ member of the series, $Na_2Ca_2Cu(SO_4)_4$, is chemically similar to itelmenite, $Na_2Mg_2Cu(SO_4)_4$, assuming the Mg-for-Ca replacement. However, the structure types of petrovite and itelmenite are different.

From the chemical point of view, petrovite demonstrates chemical and structural similarities to saranchinaite, $Na_2Cu(SO_4)_2$. The three-dimensional $[Cu(SO_4)_2]^{2-}$ anionic framework in saranchinaite is formed by corner-sharing SO_4 tetrahedra and CuO_n polyhedra with the Na^+ cations located in the cavities. In the crystal structure of petrovite, there are $[Cu_2(SO_4)_8]^{12-}$ clusters of corner-sharing Cu and S polyhedra.

The chemical formula of petrovite can be obtained from that of saranchinaite through the hypothetical reaction:

$$2Na_2Cu(SO_4)_2(\text{saranchinaite}) + CaSO_4 + 3Na_2(SO_4) \rightarrow Na_{10}CaCu_2(SO_4)_8(\text{petrovite}).$$

The reaction implies the incorporation of the ionic $CaSO_4$ and $Na_2(SO_4)$ components into the largely covalent $[Cu(SO_4)_2]^{2-}$ anionic framework with the reduction of the dimensionality of the Cu sulfate polymeric network from three (in saranchinaite) to one (in petrovite). The crystal–chemical behaviour of this kind is known as the dimensional reduction, which has been described previously in oxides and oxysalts (Alekseev *et al.*, 2007; Krivovichev, 2009; Kovrugin *et al.*, 2012).

It is of interest that both petrovite and saranchinaite contain unusual $Cu^{2+}O_7$ polyhedra. According to Siidra *et al.* (2018), the presence of the $Cu^{2+}O_7$ polyhedra is one of the potential

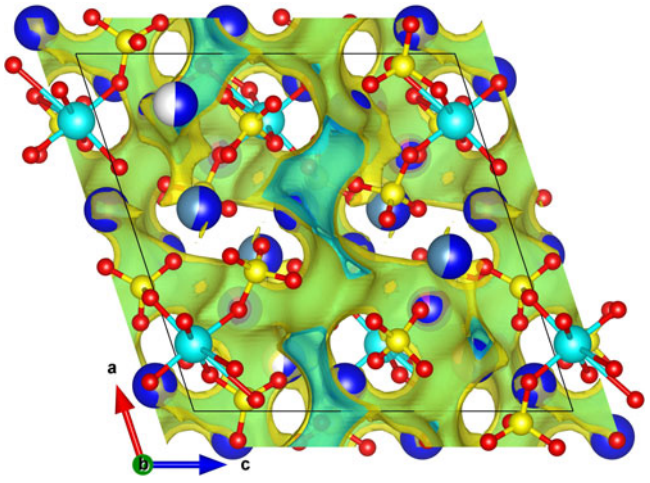

Fig. 5. The crystal structure of petrovite with the scheme of Na migration pathways. Migration pathways are calculated in *BondStr* software (Rodríguez-Carvajal, 2004).

https://doi.org/10.1180/mgm.2020.53 Published online by Cambridge University Press

reasons for the crystallisation of saranchinaite in the non-centrosymmetric space group $P2_1$. Obviously, this kind of reasoning cannot be applied to petrovite, which both contains $Cu^{2+}O_7$ polyhedra and crystallises in the centrosymmetric space group $P2_1/c$.

Many chemical compounds and materials have been synthesised based on known mineral species (see, e.g. the recent work on synthetic saranchinaite by Siidra *et al*., 2018). Therefore, the analysis of the functional properties of new minerals is important from the viewpoint of their material science applications. As the Cu^{2+}/Cu^{3+} redox potential may provide a high operating voltage (Sun *et al*., 2015), we have calculated the bond-valence energy landscape (BVEL) of petrovite using the *BondStr* software (Rodríguez-Carvajal, 2004). As a result, we have found that there are interconnected pathways for the Na^+ migration in petrovite (Fig. 5), considering a percolation energy of 1.6 eV reported for the mobility of Na^+ in polyanionic compounds (Boivin *et al*., 2017; Kovrugin *et al*., 2019). Thus, the petrovite structure type is promising as a cathode material. The theoretical capacity of petrovite based on the oversimplified formula $Na_6Cu(SO_4)_4$ ($x = 0$) is 274.5 mAh/g, but the low Cu content decreases the theoretical capacity to ~46 mAh/g.

Acknowledgements. This work was supported financially by the Russian Found of Basic Research, grant no. 18-29-12106. Technical support by the SPbSU X-ray Diffraction Centre is gratefully acknowledged.

Supplementary material. To view supplementary material for this article, please visit https://doi.org/10.1180/mgm.2020.53

References

Alekseev E.V., Krivovichev S.V., Armbruster T., Depmeier W., Suleimanov E.V., Chuprunov E.V. and Golubev A.V. (2007) Dimensional reduction in alkali metal uranyl molybdates: Synthesis and structure of $Cs_2[(UO_2)O(MoO_4)]$. *Zeitschrift für Anorganische und Allgemeine Chemie*, **633**, 1979–1984.

Boivin E., Chotard J.-N., Bamine T., Carlier D., Serras P., Palomares V., Rojo T., Iadecola A., Dupont L. and Bourgeois L. (2017) Vanadyl-type defects in tavorite-like $NaVPO_4F$: from the average long range structure to local environments. *Journal of Material Chemistry A*, **5**, 25044–25055.

Britvin S.N., Dolivo-Dobrovolsky D.V. and Krzhizhanovskaya M.G. (2017) Software for processing the X-ray powder diffraction data obtained from the curved image plate detector of Rigaku RAXIS Rapid II diffractometer. *Proceedings of the Russian Mineralogical Society*, **146**, 104–107 [in Russian].

Brown I.D. and Altermatt D. (1985) Bond-valence parameters obtained from a systematic analysis of the Inorganic Crystal Structure Database. *Acta Crystallographica*, **B41**, 244–247.

Fedotov S.A. and Markhinin Y.K. (1983) *The Great Tolbachik Fissure Eruption*. Cambridge University Press, New York.

Filatov S.K., Karpov G.A., Shablinskii A.P., Krivovichev S.V., Vergasova L.P. and Antonov A.V. (2013) Ivsite, $Na_3H(SO_4)_2$, a new mineral from volcanic exhalations of fumaroles of the fissure Tolbachik eruption of the 50th anniversary of the Institute of Volcanology and Seismology, Far East Branch, Russian Academy of Sciences. *Doklady Earth Sciences*, **468**, 632–635.

Filatov S.K., Shablinskii A.P., Vergasova L.P., Saprikina O.U, Bubnova R.S, Moskaleva S.V. and Belousov A.B. (2019) Belomarinaite $KNa(SO_4)$: a new sulfate from 2012–2013 Tolbachik Fissure eruption, Kamchatka Peninsula, Russia. *Mineralogical Magazine*, **83**, 569–575.

Filatov, S.K., Shablinskii, A.P., Vergasova, L.P., Krivovichev, S.V. and Moskaleva, S.V. (2020) Petrovite, IMA 2018-149b. CNMNC Newsletter No. 53; *Mineralogical Magazine*, **84**, https://doi.org/10.1180/mgm.2020.5

Gorelova L.A., Vergasova L.P., Krivovichev S.V., Avdontseva E.Y., Moskaleva S.V., Karpov G.A. and Filatov S.K. (2016) Bubnovaite, $K_2Na_8Ca(SO_4)_6$, a new mineral species with modular structure from the Tolbachik volcano, Kamchatka peninsula, Russia. *European Journal of Mineralogy*, **28**, 677–686.

Hawthorne F.C., Krivovichev S.V. and Burns P.C. (2000) The crystal chemistry of sulfate minerals. Pp. 1–112 in: *Sulfate minerals – Crystallography, Geochemistry and Environmental Significance* (C.N. Alpers, J.L. Jambor and D.K. Nordstrom, editors). Reviews in Mineralogy & Geochemistry, **40**. Mineralogical Society of America and the Geochemical Society, Washington, DC.

Karpov G.A., Krivovichev S.V., Vergasova L.P., Chernyat'eva A.P., Anikin L.P., Moskaleva S.V. and Filatov S.K. (2013) Oxysulfates of copper, sodium, and potassium in the lava flows of the 2012–2013 Tolbachik Fissure Eruption. *Journal of Volcanology and Seismology*, **7**, 362–370.

Kovrugin V.M., Gurzhiy V.V. and Krivovichev S.V. (2012) Structural topology and dimensional reduction in uranyl oxysalts: eight novel phases in the methylamine–$(UO_2)(NO_3)_2$–H_2SeO_4–H_2O system. *Structural Chemistry*, **23**, 2003–2017.

Kovrugin V.M., Nekrasova D.O., Siidra O.I., Mentre O., Masquelier C., Stefanovich S.Y. and Colmont M. (2019) Mineral-inspired crystal growth and physical properties $Na_2Cu(SO_4)_2$ and review of $Na_2M(SO_4)_2(H_2O)_x$ ($x = 0$–6) Compounds. *Crystal Growth and Design*, **19**, 1233–1244.

Krivovichev S.V. (2009) *Structural Crystallography of Inorganic Oxysalts*. Oxford University press, Oxford, UK.

Mandarino J.A. (1981) The Gladstone-Dale relationship: Part IV. The compatibility concept and its application. *The Canadian Mineralogist*, **19**, 441–450.

Nadeem M.A., Bhadbhade M., Bircher R. and Stride J.A. (2010) Three isolated structural motifs in one crystal: penetration of two 1D chains through large cavities within 2D polymeric sheets. *CrystEngComm*, **12**, 1391–1393.

Nazarchuk E.V., Siidra O. I., Agakhanov A.A., Lukina E.A., Avdontseva E. Y. and Karpov G. A. (2018) Itelmenite, $Na_2CuMg_2(SO_4)_4$, a new anhydrous sulphate mineral from the Tolbachik volcano. *Mineralogical Magazine*, **82**, 1233–1241.

Pekov I.V., Shchipalkina N.V., Zubkova N.V., Gurzhiy V.V., Agakhanov A.A., Belakovskiy D.I., Chukanov N.V., Lykova I.S., Vigasina M.F., Koshlyakova N.N., Sidorov E.G. and Giester G. (2019) Alkali sulfates with aphthitalite-like structures from fumaroles of the Tolbachik volcano, Kamchatka, Russia. I. Metathénardite, a natural high-temperature modification of Na_2SO_4. *The Canadian Mineralogist*, **57**, 885–901.

Pekov I.V., Agakhanov A.A., Zubkova N.V., Koshlyakova N.N., Shchipalkina N.V., Sandalov F.D., Yapaskurt V.O., Turchkova A.G. and Sidorov E.G. (2020) Oxidizing-type fumarolic systems of the Tolbachik volcano – a mineralogical and geochemical unique. *Russian Geology and Geophysics*, https://doi.org/10.2205/2013ES000529

Petříček V., Dusek M. and Palatinus L. (2006) *Jana2006. The Crystallographic Computing System*. Institute of Physics, Academy of Sciences of the Czech Republic, Prague.

Petrov T.G. (2014) Separation-mixing as a model of composition evolution of any nature. *Journal on Systemics, Cybernetics and Informatics*, **12**, 76–81.

Petrov T.G., Treywus E.B. and Kasatkin A.P. (1969) *Crystal Growth from Solution*. Plenum Publishing Corporation., New York 106 p.

Petrov T.G., Andriyanets-Buyko A. A., Moshkin, S. V. (2012) A two-parameter alphabet for coding structural–chemical information and its systematization (using the example of tourmaline). *Automatic Documentation and Mathematical Linguistics*, **46**, 40–49.

Petrov T.G., Protopopov E.N. and Shuyskiy A.V. (2013) Decorative grown malachite. Nature and technology. *Russian Journal of Earth Sciences*, **13**, https://doi.org/10.2205/2013ES000529

Rodríguez-Carvajal J. (2004) *The program BondStr and its GUI GBondStr*. http://www.ccp14.ac.uk/ccp/web-mirrors/plotr/BondStr/Bond_Str.htm

Shablinskii A.P., Filatov S.K., Vergasova L.P., Moskaleva S.V., Avdontseva E.Y. and Bubnova R.S. (2020) Dobrovolskyite, IMA 2019-106, in: CNMNC Newsletter 54, *Mineralogical Magazine*, **84**, 359–365.

Shchipalkina N.V., Pekov I.V., Chukanov N.V., Zubkova N.V., Belakovskiy D.I., Koshlyakova N.N., Britvin S.N., Sidorov E.G. and Vozchikova S.A. (2020) Alkali sulfates with aphthitalite-like structures from fumaroles of the Tolbachik volcano, Kamchatka, Russia. II. A new mineral,

natroaphthitalite, and new data on belomarinaite. *The Canadian Mineralogist*, **58**, 167–181.

Siidra O.I., Nazarchuk E.V., Zaitsev A.N., Lukina E.A., Avdontseva E.Y., Vergasova L.P., Vlasenko N.S., Filatov S.K. and Karpov G.A. (2017) Copper oxosulphates from fumaroles of Tolbachik volcano: puninite, $Na_2Cu_3O(SO_4)_3$ – a new mineral species and structure refinements of kamchatkite and alumoklyuchevskite. *European Journal of Mineralogy*, **29**, 499–510.

Siidra O.I., Lukina E.A., Nazarchuk E.V., Depmeier W., Bubnova R.S., Agakhanov A.A., Avdontseva E.Y., Filatov S.K. and Kovrugin V.M. (2018) Saranchinaite, $Na_2Cu(SO_4)_2$, a new exhalative mineral from Tolbachik volcano, Kamchatka, Russia, and a product of the reversible dehydration of kröhnkite, $Na_2Cu(SO_4)_2(H_2O)_2$. *Mineralogical Magazine*, **82**, 257–274.

Siidra O.I., Nazarchuk E.V., Zaitsev A.N. and Vlasenko N.S. (2020) Koryakite, $NaKMg_2Al_2(SO_4)_6$, a new NASICON-related anhydrous sulfate mineral from Tolbachik volcano, Kamchatka, Russia. *Mineralogical Magazine*, **84**, 283–287.

Sun M., Rousse G., Abakumov A.M., Saubanère M., Doublet M.L., Rodríguez-Carvajal J., Van Tendeloo G. and Tarascon J.M. (2015) $Li_2Cu_2O(SO_4)_2$: A Possible Electrode for Sustainable Li-Based Batteries Showing a 4.7 V Redox Activity vs Li^+/Li^0. *Chemistry of Materials*, **27**, 3077–3087.

Vergasova L.P. and Filatov S.K. (2012) New mineral species in products of fumarole activity of Great Tolbachik fissure eruption. *Journal of Volcanology and Seismology*, **6**, 281–289.

Vergasova L.P. and Filatov S.K. (2016) A study of volcanogenic exhalation mineralization. *Journal of Volcanology and Seismology*, **10**, 71–85.

Yoshiasa A., Yagyu G., Ito T., Yamanaka T. and Nagai T. (2000) Crystal structure of the high pressure phase(II) in $CuGeO_3$. *Zeitschrift für Anorganische und Allgemeine Chemie*, **626**, 36–41.

https://doi.org/10.1180/mgm.2020.53 Published online by Cambridge University Press